The control of tissue architecture over nuclear organization is crucial for epithelial cell fate

Gurushankar Chandramouly[1], Patricia C. Abad[1], David W. Knowles[2] and Sophie A. Lelièvre[1,*]

[1]Department of Basic Medical Sciences and Cancer Center, Purdue University, 625 Harrison Street, West Lafayette, IN 47907-2026, USA
[2]Life Sciences Division, Lawrence Berkeley National Laboratory, 1 Cyclotron Road, Berkeley, CA 94720, USA
*Author for correspondence (e-mail: lelievre@purdue.edu)

Accepted 23 February 2007
Journal of Cell Science 120, 1596-1606 Published by The Company of Biologists 2007
doi:10.1242/jcs.03439

Summary

The remodeling of nuclear organization during differentiation and the dramatic alteration of nuclear organization associated with cancer development are well documented. However, the importance of tissue architecture in the control of nuclear organization remains to be determined. Differentiation of mammary epithelial cells into functional tissue structures, in three-dimensional culture, is characterized by a specific tissue architecture (i.e. a basoapical polarity axis), cell cycle exit and maintenance of cell survival. Here we show that induction of partial differentiation (i.e. basal polarity only, cell cycle exit and cell survival) by epigenetic mechanisms in malignant breast cells is sufficient to restore features of differentiation-specific nuclear organization, including perinucleolar heterochromatin, large splicing factor speckles, and distinct nuclear mitotic apparatus protein (NuMA) foci. Upon alteration of nuclear organization using an antibody against NuMA, differentiated non-neoplastic cells undergo apoptosis, whereas partially differentiated malignant cells enter the cell cycle. Non-neoplastic cells cultured under conditions that prevent the establishment of apical polarity also enter the cell cycle upon NuMA antibody treatment. These findings demonstrate that the differentiation status rather than the non-neoplastic or neoplastic origin of cells controls nuclear organization and suggest a link between nuclear organization and epigenetic mechanisms dictated by tissue architecture for the control of cell behavior.

Key words: Mammary epithelial differentiation, Nuclear structure, Proliferation, Tumor reversion, NuMA, Three dimensional cell culture

Introduction

Epithelial tissue differentiation is accompanied by the maintenance of both cell survival and growth arrest. The architecture of differentiated epithelial tissues, which is characterized by a basoapical polarity axis (Bilder and Perrimon, 2000; O'Brien et al., 2001), is a supreme epigenetic pathway (i.e. unrelated to changes in DNA sequence) in the maintenance of functional differentiation (Plachot and Lelièvre, 2004; Nelson and Bissell, 2006). In glandular epithelia, the basal pole of the polarity axis is against the extracellular basement membrane, and the apical pole of the polarity axis is next to the lumen. Each of these cellular poles includes specific adhesion complexes (Caplan, 1997; Plachot and Lelièvre, 2003): hemidesmosomes are located at the basal pole, where they connect cells to the basement membrane; and tight junctions are located towards the apical pole, where they seal the intercellular space and maintain basoapical polarity and, thus, proper tissue function (e.g. vectorial secretion into the central lumen) by creating a barrier between basolateral and apical domains (Rodriguez-Boulan and Nelson, 1989; Cereijido et al., 1998). Hemidesmosomes play a crucial role in epithelial tissue homeostasis by maintaining differentiation and cell survival (Dowling et al., 1996; Weaver et al., 2002) and tight junctions are involved in the control of cell proliferation (Balda et al., 2003; Gonzalez-Mariscal and Nava, 2005).

Besides the basoapical polarity axis, another structural feature characteristic of epithelial differentiation is the organization of the cell nucleus. The specific location of both nonchromatin and chromatin structures within the cell nucleus, which is referred to as higher order nuclear structure, has been shown to change dramatically upon differentiation. Nonchromatin splicing factor speckles have been observed to be larger in differentiated cells compared with nondifferentiated cells (Lelièvre et al., 1998; Gribbon et al., 2002). Heterochromatin domains or chromodomains have been found to localize to different nuclear areas in differentiated cells compared with nondifferentiated cells (Manuelidis, 1985; Martou and De Boni, 2000). Using the three-dimensional (3D) cell culture model of human mammary epithelial cell (HMEC) differentiation into glandular structures (acini) – where cells first proliferate, then exit the cell cycle and undergo basoapical polarization (Petersen et al., 1992; Weaver et al., 2002; Plachot and Lelièvre, 2004; Lelièvre and Bissell, 2005) – we have identified certain modifications in higher order nuclear structure associated with cell cycle exit (Lelièvre et al., 1998; Kaminker et al., 2005), and additional modifications at later stages of differentiation (Lelièvre et al., 1998). Moreover, we have shown that disrupting higher order nuclear structure by altering the distribution of a specific nuclear protein, either upon expression of its truncated form [e.g. truncated TIN2; truncated nuclear mitotic apparatus protein (NuMA)] or introduction of an antibody against the protein (e.g. antiNuMA antibody), leads to a lack of proper polarity and the maintenance of cell cycle activity, in the case of TIN2

(Kaminker et al., 2005), and the alteration of the basement membrane, a crucial component of basal polarity, in the case of NuMA (Lelièvre et al., 1998; Abad et al., 2007). It has long been recognized that the organization of the cell nucleus appears quite different in malignant cells compared with non-neoplastic cells (reviewed by Zink et al., 2004). However, the reasons for such differences are not known. Here we have asked whether the dramatic changes in nuclear organization observed in cancer cells are associated with the loss of epithelial tissue architecture.

Using different models of mammary acinar differentiation in 3D culture, we show that the differentiation-specific organization of certain markers of higher order nuclear structure is lost in malignant cells arranged into nonpolarized nodules; however, in malignant cells induced to form growth-arrested and basally polarized (but not apically polarized) acinus-like structures (i.e. structures with partial differentiation), these markers of higher order nuclear structure are organized similarly to those seen in phenotypically normal acini. Alteration of higher order nuclear structure using antibodies against the nuclear structural protein NuMA is associated with apoptosis in non-neoplastic cells and entrance into the cell cycle in partially differentiated malignant cells. We further show that altered tissue architecture characterized by the absence of apical polarity, prior to antibody induced-alteration of nuclear organization, is a determining factor for entry into the cell cycle.

Results

Reversion of malignant HMECs in 3D culture is accompanied by the establishment of features of higher order nuclear structure

Concentration of heterochromatin at the nucleolar and/or nuclear periphery and formation of enlarged splicing factor speckles are nuclear features of differentiation in several cell types, including mammary epithelial cells (Manuelidis, 1985; Antoniou et al., 1993; Chaly and Munro, 1996; Lelièvre et al., 1998; Martou and De Boni, 2000; Gribbon et al., 2002; Beil et al., 2002; Garagna et al., 2004; Abad et al., 2007). To assess whether features of nuclear organization that are characteristic of mammary acinar differentiation are lost in breast cancer cells, we cultured non-neoplastic S1 cells (Briand et al., 1987) and S1-derived malignant T4-2 cells (Briand et al., 1996) in Matrigel^{TM} in 3D for 10 days. Upon this culture period we verified that S1 cells had formed fully differentiated acini. HMEC acinar differentiation in 3D culture is commonly determined by cell cycle exit (i.e. no Ki67 expression) and the correct distribution of markers of basolateral polarity (e.g. collagen IV uninterrupted around the acinus, hemidesmosome component α6-integrin at the basal cell membrane, β-catenin at cell-cell junctions) and apical polarity (e.g. mucin-1 at the lateroapical and apical cell membranes) (Petersen et al., 1992; Weaver et al., 1997; Plachot and Lelièvre, 2004; Lelièvre and Bissell, 2005) (Fig. 1A,B). We also verified that tumor-like nodules formed by malignant cells showed cell cycle activity and displayed disorganized basolateral and apical polarity markers (Petersen et al., 1992; Weaver et al., 1997; Wang et al., 1998; Lelièvre and Bissell, 2005) (Fig. 1A,B). Results from visual scoring of the distribution of differentiation markers show that ~74% of S1 acini are completely surrounded by collagen IV versus ~8% of T4-2 nodules. As illustrated in Fig. 1A, the correct distribution of α6-integrin and mucin-1 is found in ~73% and ~15% of S1 acini, respectively, versus ~10% and 0% of T4-2 tumor nodules, respectively. [Note that Mucin-1 is not detected in the remaining 85% of S1 acini. Our hypothesis is that it may be removed from the lumen during the immunostaining process.]

The organization of the cell nucleus was studied by assessing the distribution of markers specific for chromatin and nonchromatin compartments. Immunostaining for heterochromatin markers histone 4 methylated on lysine 20 (H4K20m) and histone 3 methylated on lysine 9 (H3K9m) (Lachner et al., 2001; Fischle et al., 2003; Schotta et al., 2004) revealed their concentration around the nucleolus in S1 acinar cells. By contrast, these markers appeared mostly as small foci throughout the nuclear space, without any remarkable concentration in specific nuclear areas, in malignant T4-2 cells (Fig. 1C). Nuclear proteins such as promyelocytic leukemia (PML) protein (Zhong et al., 2000), nuclear shell protein lamin B (Moir et al., 1994), splicing factor SC35 (Fay et al., 1997) and NuMA (Compton and Cleveland, 1994; Abad et al., 2004) have been proposed to play a crucial role in nuclear structure, possibly by organizing other nuclear components, including chromatin (Barboro et al., 2002; Shumaker et al., 2003; Abad et al., 2004; Hall et al., 2006; Abad et al., 2007). Some of these markers are known to adopt a specific organization in differentiated cells. Visual observation has revealed the formation of distinct and large NuMA foci upon breast acinar differentiation (Lelièvre et al., 1998). The PML protein distribution changes from diffuse to distinct foci upon differentiation of leukaemic cells (Andre et al., 1996). Splicing factor speckles are enlarged in differentiated erythroid cells compared with those in neoplastic cells (Antoniou et al., 1993). Upon comparison of differentiated S1 and malignant T4-2 cells for NuMA distribution on a per cell basis using the local bright feature (LBF)-radial analysis (Knowles et al., 2006), we have found that NuMA was typically organized into distinct domains concentrated in mid-nucleus in S1 acini, whereas its distribution appeared diffuse (i.e. no concentration of staining foci in specific areas of the cell nucleus) in T4-2 tumor nodules (Knowles et al., 2006) (Fig. 1D). Visual observation did not reveal striking differences in PML distribution when comparing breast malignant T4-2 cells and non-neoplastic differentiated S1 cells. However, the distribution of SC35, a marker of splicing factor speckle organization consisted of a few large domains often arranged as a ring in mid-nucleus in acinar S1 cells, whereas speckles were smaller and distributed throughout the nuclear space in malignant T4-2 cells (Fig. 1D). Interestingly lamin B, an integral protein of the inner nuclear membrane, remained peripheral in both cell types, but clearly revealed the twisted nuclear shape in malignant cells. Thus, tumor nodule formation is accompanied by dramatic alterations in important nuclear structural features when compared with acinar differentiation.

We reasoned that if the features of nuclear organization observed in acinar S1 cells depend on differentiation rather than on the non-neoplastic nature of the cells, induction of phenotypic reversion in malignant cells should lead to the restoration of the same features. Malignant T4-2 cells were induced to differentiate according to protocols used previously (Weaver et al., 1997; Wang et al., 1998; Wang et al., 2002) and the distribution of the set of proteins described above was

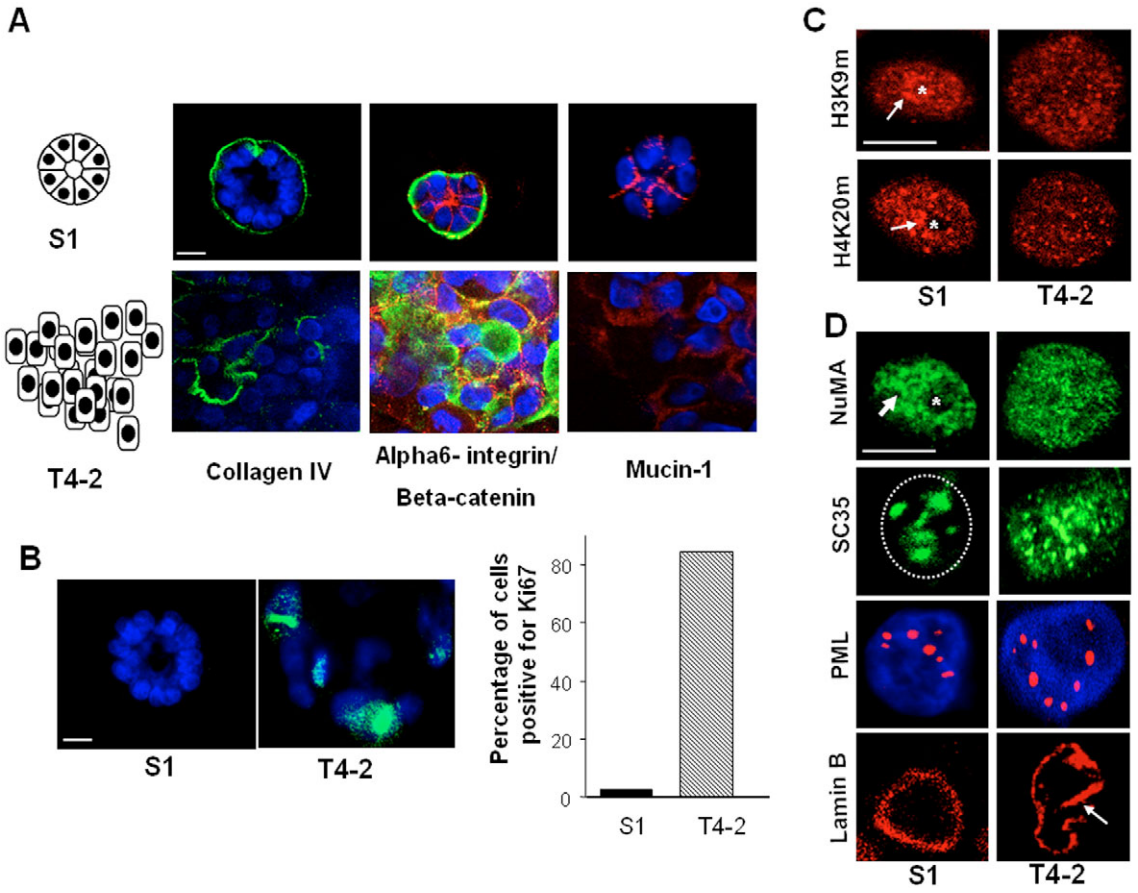

Fig. 1. Tumor nodules display altered tissue polarity and nuclear organization compared with acini formed by non-neoplastic cells. S1 and T4-2 cells were cultured in 3D in the presence of Matrigel™ for 10 days and labeled for differentiation markers collagen IV, α6-integrin, β-catenin, mucin-1 and Ki-67, and markers of nuclear organization H3K9m, H4K20m, NuMA, SC35, PML and lamin B. (A) Immunostaining for basal polarity markers collagen IV (green) and α6-integrin (green), lateroapical polarity marker β-catenin (red), and apical polarity marker mucin-1 (red) in acinar S1 cells (top panel) and malignant T4-2 cells (bottom panel). Drawings show the organization of S1 and T4-2 cells after 10 days of 3D culture; nuclei are represented in black. (B) Immunostaining for cell cycle marker Ki67 (green). Nuclei are counterstained with DAPI (blue). Bar graph shows the percentage of cells in the cell cycle based on Ki67 expression. (C) Organization of heterochromatin markers H3K9m (red) and H4K20m (red) in the nuclei of acinar (S1) and malignant (T4-2) cells. Arrows indicate the concentration of H3K9m and H4K20m around the nucleolus (*) in differentiated cells. (D) Organization of coiled-coil protein NuMA (green), splicing factor speckle marker SC35 (green), PML (red, with DAPI-counterstained nuclei in blue) and lamin B (red) in the nuclei of acinar (S1) and malignant (T4-2) cells. The arrowhead indicates the formation of enlarged NuMA foci in mid-nucleus in S1 cells. SC35 is organized into large domains in the nucleus of S1 cells (dotted line delineates the cell nucleus). The arrow points to the twisted shape of the malignant nucleus as shown by lamin B staining. Bars, 5 μm.

analyzed. Reversion protocols restore aspects of phenotypically normal tissue architecture, and cellular growth arrest and survival although the genotype remains the same as in malignant cells (Weaver et al., 1997). Malignant T4-2 cells were treated with reverting agent AG1478, an inhibitor of the EGFR pathway and cultured in 3D for 10 days to induce differentiation (Weaver et al., 1997; Wang et al., 1998). We verified that the multicellular structures formed by reverted T4-2 (RT4-2) cells, referred to as spheroids, exited the cell cycle, as shown by the absence of Ki67 expression, and displayed basolateral polarity as shown by the distribution of the basement membrane component collagen IV (correctly organized in ~78% of spheroids) and adhesion complex protein α6-integrin (correctly organized in ~60% of spheroids) (Fig. 2A,B). However, spheroids formed by RT4-2 cells lacked proper apical polarity. All the spheroids in which mucin-1 was detected (~12% of the spheroids) displayed a basal or peripheral location of the staining for mucin-1 (compare RT4-2 spheroids Fig. 2A with S1 acini Fig. 1A). This particular location of mucin-1 has been referred to as inverted polarity (Gudjonsson et al., 2003). Thus, with the exception of mucin-1, a majority of RT4-2 spheroids displayed a correct organization of the differentiation markers analyzed.

Visual scoring revealed that higher order nuclear organization in a significant portion of the RT4-2 cell population was characterized by a concentration of heterochromatin markers H4K20m and H3K9m at the nucleolar periphery, which is similar to the organization seen in S1 acinar cells. By contrast, T4-2 cells incubated with DMSO, the vehicle for AG1478, displayed smaller heterochromatin domains dispersed throughout the nuclear volume similarly to the distribution found in control T4-2 cells

(compare Fig. 2C with Fig. 1C; Fig. 2E), the distribution of SC35 into a few large domains was also restored in a significant portion of the RT4-2 cell population (Fig. 2D,E). Application of the radial-LBF analysis to measure NuMA distribution demonstrated that cell populations could be subdivided into cells with a high density of foci-like distribution of NuMA, characteristic of differentiation, and cells with a flat distribution of NuMA, corresponding to nondifferentiated stages. Classification into these two groups allowed us to determine the ratio of numbers of cells with differentiation-like and cells with nondifferentiation-like distributions of NuMA in differentiated (S1), malignant (T4) and reverted (RT4-2) cell populations. Analyses of the results showed that there was no statistical difference between populations of RT4-2 cells and S1 cells, based on NuMA distribution. Whereas, there was a statistically significant difference between RT4-2 and T4-2 cell populations, based on NuMA distribution (Fig. 2D,E).

To verify that the features of higher order nuclear structure observed in RT4-2 cells were not specific to AG1478 treatment, we induced the phenotypic reversion of T4-2 cells with another agent, LY294002 (Wang et al., 2002), which acts as an inhibitor of the phosphoinositide (PI) 3-kinase pathway. LY294002-induced reversion was accompanied by the proper organization of basolateral polarity markers collagen IV, α6-integrin, and β-catenin, but not the apical polarity marker mucin-1 (Fig. 3A). In LY294002-induced RT4-2 cells, the distribution of markers of higher order nuclear structure, as

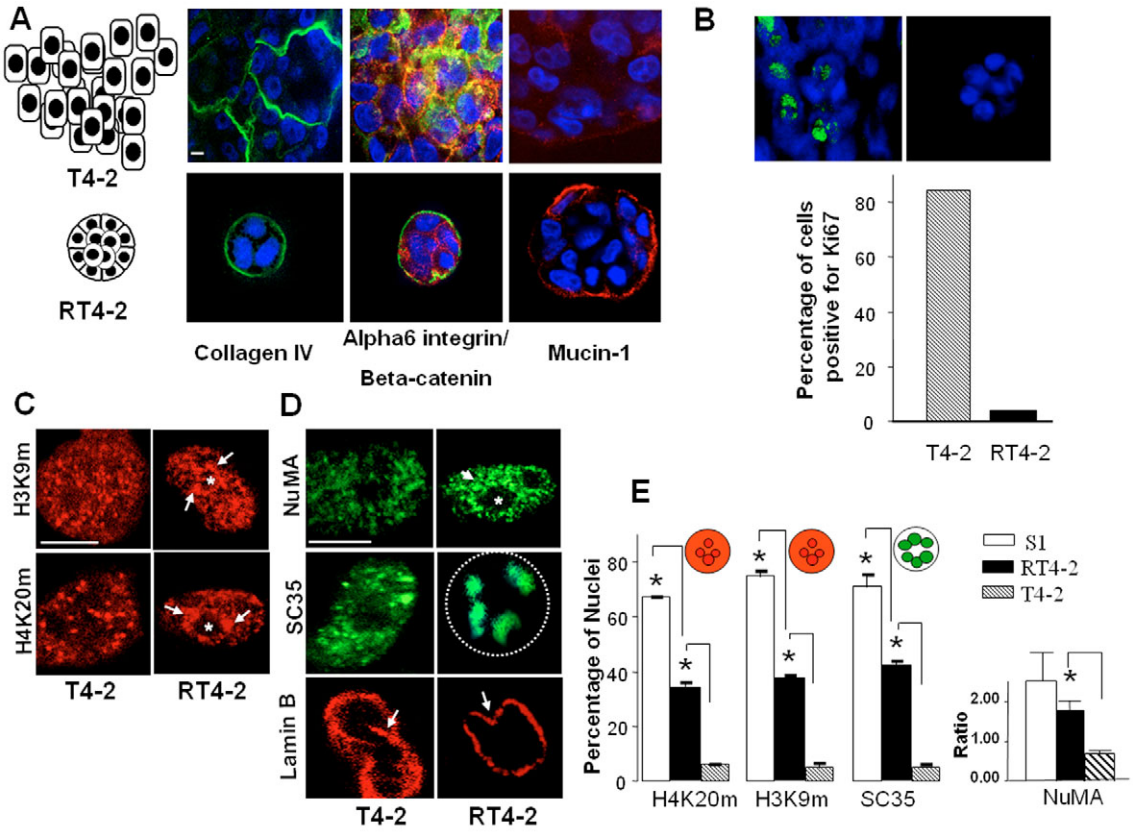

Fig. 2. AG1478-induced phenotypic reversion of malignant cells is accompanied by partial tissue polarity and the re-establishment of the organization of markers of higher order nuclear structure. Malignant T4-2 cells were treated either with the reverting agent AG1478 or vehicle DMSO for 10 days in 3D culture in the presence of Matrigel™ and labeled for differentiation markers collagen IV, α6-integrin, β-catenin, mucin-1, and Ki67, and for nuclear proteins H3K9m, H4K20m, NuMA, SC35 and lamin B. (A) Immunostaining for basal polarity markers collagen IV (green) and α6-integrin (green), lateroapical polarity marker β-catenin (red), and apical polarity marker mucin-1 (red) in malignant T4-2 cells (top panel) and reverted RT4-2 cells (bottom panel). Drawings represent the organization of T4-2 and RT4-2 cells after 10 days of 3D culture. Nuclei are represented in black. (B) Immunostaining for cell cycle marker Ki67 (green). Nuclei are counterstained with DAPI (blue). Bar graph shows the percentage of cells in the cell cycle based on Ki67 expression. (C) Organization of heterochromatin markers H3K9m (red) and H4K20m (red) in the nuclei of malignant (T4-2) and reverted (RT4-2) cells. Arrows indicate the concentration of H3K9m and H4K20m around the nucleolus (*) in differentiated cells. (D) Organization of coiled-coil protein NuMA (green), splicing factor speckle marker SC35 (green), and lamin B (red) in the nuclei of malignant (T4-2) and reverted (RT4-2) cells. The arrowhead indicates the formation of enlarged NuMA foci in mid-nucleus in RT4-2 cells. SC35 is organized into large domains in the nucleus of RT4-2 cells (a dotted line delineates the cell nucleus). The arrows point to the twisted shape, as shown by lamin B staining, of the nucleus in malignant and reverted cells. (E) Left histogram: Percentage of nuclei in S1 acini, T4-2 tumor nodules, and RT4-2 spheroids with nuclear proteins displaying a distribution characteristic of acinar differentiation. Drawings show the distributions of H4K20m, H3K9m and SC35 representative of acinar differentiation. Right histogram: ratios of cells with differentiation-like distribution of NuMA over cells with nondifferentiation-like distribution of NuMA in the S1, RT4-2 and T4-2 populations.*P<0.01. Bars, 5 μm.

shown by H4K20m, NuMA and SC35 staining, was similar to that observed in AG1478-induced RT4-2 cells (compare Fig. 3B and Fig. 2C,D). Control and DMSO-treated T4-2 3D cultures usually display a number of small nodules in addition to the large tumor-like nodules at day 10. Therefore, we confirmed that the specific features of nuclear organization observed in acinar S1 cells and RT4-2 cells did not occur in malignant cells that formed small tumor nodules. Results show that although certain nodules formed by DMSO-treated T4-2 cells have sizes similar to RT4-2 spheroids, their architecture is disorganized, as in larger tumor nodules, and the distribution of markers of higher order nuclear structure in these small tumor nodules is also similar to that seen in larger tumor nodules (compare Fig. 3A,B, left panels and Fig. 2A,C,D).

We conclude that the phenotypic reversion of malignant cells, characterized by the formation of growth-arrested and basolaterally polarized multicellular spheroids, is accompanied by the reorganization of markers of higher order nuclear structure, despite the existence of DNA abnormalities (Weaver et al., 1997) and an altered nuclear shape.

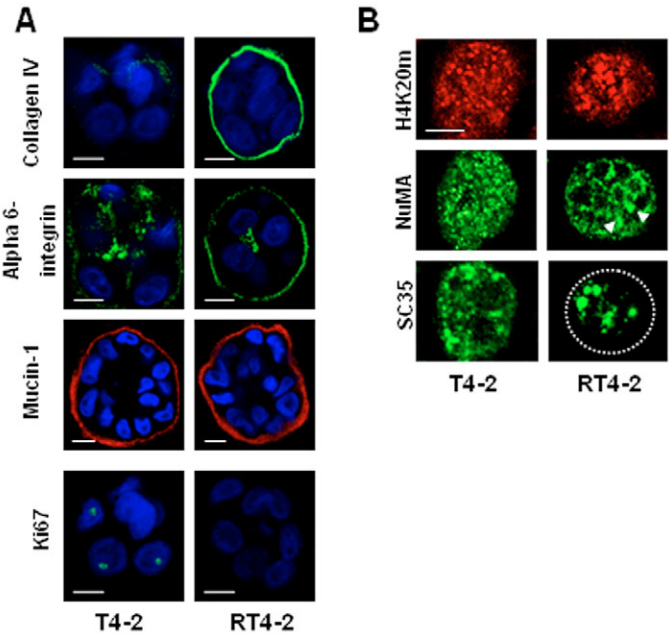

Fig. 3. LY294002 induced-phenotypic reversion of malignant cells is accompanied with the re-establishment of basal polarity and higher order nuclear structure. Malignant T4-2 cells were treated either with the reverting agent LY294002 or vehicle DMSO for 10 days in 3D culture in the presence of Matrigel™ and labeled for differentiation markers collagen IV, α6-integrin, mucin-1 and Ki67, and nuclear proteins H4K20m, NuMA and SC35. (A) Immunostaining for basal polarity markers collagen IV (green) and α6-integrin (green), apical polarity marker mucin-1 (red), and proliferation marker Ki67 (green) in malignant (T4-2) cells (small tumor nodules are shown) and reverted (RT4-2) cells. Nuclei are counterstained with DAPI (blue). (B) Organization of heterochromatin marker H4K20m (red), coiled-coil protein NuMA (green; arrowheads indicate the presence of enlarged foci in mid-nucleus) and splicing factor speckle marker SC35 (green) in the nuclei of malignant (T4-2) and reverted (RT4-2) cells. The dotted line delineates the cell nucleus. Bars, 5 μm.

Alteration of nuclear organization in reverted tumor cells leads to the loss of differentiation

The re-establishment of features of nuclear organization characteristic of differentiation in RT4-2 cells in 3D culture raises the question whether such reorganization is important for the differentiation stage observed in these cells. We had shown previously that the distribution of NuMA observed in S1 acini was crucial for the maintenance of acinar differentiation (Lelièvre et al., 1998). Indeed, upon introduction of antiNuMA-C-terminus (CT) antibodies in live acinar cells, endogenous NuMA became diffusely distributed and, subsequently, acinar differentiation became altered, as shown by the absence of complete collagen IV staining at the periphery of the acini (Lelièvre et al., 1998; Abad et al., 2007). We further showed that NuMA played a crucial role in acinar differentiation by controlling higher order organization of chromatin measured by the distribution of chromatin markers H4K20m and acetyl-H4 (Abad et al., 2007). We reasoned that, similarly, if the reorganization of NuMA observed in RT4-2 spheroids is linked to differentiation, perturbing NuMA distribution in these spheroids should alter their differentiation stage. To do so, we used the antiNuMA antibody-based method that enables us to alter NuMA in already formed multicellular structures in 3D culture. S1, T4-2 and RT4-2 cells were cultured in 3D for 10 days to induce the formation of acini, tumor nodules, and spheroids, respectively, and incubated with antiNuMA antibodies or control nonspecific immunoglobulins (IgGs) for 4 days following a 30-second permeabilization with digitonin, according to a procedure used previously (Lelièvre et al., 1998; Abad et al., 2007). As shown before for S1 acinar cells (Lelièvre et al., 1998), the distribution of endogenous NuMA was diffuse in RT4-2 cells incubated with antiNuMA antibody (~82% of S1 cells and ~78% of RT4-2 cells treated with antiNuMA antibody showed a diffuse distribution of NuMA in these experiments compared with ~11% of cells treated with nonspecific IgGs). Whereas, no change could be detected in T4-2 cells in which NuMA distribution remained diffuse (Fig. 4A). As expected, S1 cell cultures showed a 3.2-fold increase in acini with incomplete collagen IV staining upon incubation with antiNuMA antibody (14.2% of acini with incomplete collagen IV staining in IgG-treated cultures compared to 46% of acini with incomplete collagen IV staining in antiNuMA antibody-treated cultures). Similarly, there was a 2.4-fold increase in RT4-2 spheroids with incomplete collagen IV staining upon incubation with antiNuMA antibody (22% of acini with incomplete collagen IV staining in IgG-treated cultures compared to 47% of acini with incomplete collagen IV staining in antiNuMA antibody-treated cultures) (Fig. 4B). Although T4-2 nodules are not commonly surrounded by a basement membrane, T4-2 cells often secrete high amounts of collagen IV (see Fig. 1). The percentage of nodules showing a significant amount of collagen IV did not change in T4-2 cell cultures incubated with antiNuMA antibody compared with cultures incubated with nonspecific IgGs (Fig. 4B).

The presence of an intact basement membrane is crucial for the survival of normal epithelial tissue (Pullan et al., 1996; Chrenek et al., 2001); therefore, apoptosis rate was measured in S1, T4-2 and RT4-2 cells incubated with nonspecific IgGs and with antiNuMA antibody. There was a fourfold increase in apoptosis rate in S1 cells incubated with antiNuMA antibody. However, upon antibody treatment, neither T4-2 cells nor RT4-

2 cells showed an increase in apoptosis rate (Fig. 4C). Since cell proliferation may be an alternative to apoptosis upon alteration of basement membrane components (Lochter et al., 1998; Ortega and Werb, 2002), we also assessed the percentage of cells in the cell cycle. RT4-2 spheroids incubated with antiNuMA antibody had a fourfold increase in the percentage of cells in the cell cycle; incubation with antiNuMA antibody also triggered the formation of mitotic spindles (Fig. 4D). By contrast, upon antibody treatment, neither S1 acini nor T4-2 tumor nodules showed an increase in the percentage of cells in the cell cycle (Fig. 4D). Thus, although the nuclear organization of NuMA plays a role in the maintenance of differentiation in both S1 acini and RT4-2 spheroids, the response to NuMA alteration differs between non-neoplastic and reverted cells.

The cell behavior induced by the alteration of NuMA is controlled by tissue polarity

The reason that RT4-2 cells re-enter the cell cycle upon NuMA antibody treatment could be associated with either their malignant status or their stage of differentiation. RT4-2 spheroids do not display mucin-1 at the apical cell membranes (Figs 2, 3), which indicates that substructures essential for the establishment of apical polarity, a major aspect of the differentiation of epithelial tissues (Aijaz et al., 2006), are probably perturbed. The formation of tight junctions is paramount for the establishment of apical polarity in epithelial tissues. Interestingly, tight junctions have been involved in the control of cell proliferation (Balda et al., 2003; Gonzalez-Mariscal and Nava, 2005). ZO-1 is a central regulator of tight junction formation (Mitic et al., 1999; Ryeom et al., 2000) and it is present at the apical side of acini in normal breast epithelial tissue (Martin et al., 2004) and in 3D culture (Plachot and Lelièvre, 2004). To determine the status of tight junctions in the different phenotypes studied above, we immunostained for ZO-1 in S1, T4-2 and RT4-2 cells cultured under 3D conditions for 10 days. ZO-1 was apically distributed in acinar S1 cells (~72% of acini show an apical concentration of ZO-1) and it was located throughout the cytoplasm in all malignant T4-2 cells. ZO-1 was absent from the apical pole of ~98% of RT4-2 spheroids, which confirmed that RT4-2 spheroids have an altered architecture (Fig. 5A).

To test whether the lack of proper tissue polarity could influence the response of non-neoplastic cells to NuMA alteration, we used a particular cell culture procedure to produce growth-arrested and basally polarized (but not apically polarized) acinus-like structures. S1 cells were cultured in the presence of collagen I for 9 days, to induce the formation of growth-arrested multicellular structures of sizes similar to acini formed in Matrigel™, but lacking basoapical polarity (Weaver et al., 2002; Gudjonsson et al., 2003). Then, we replated collagen I-induced S1 multicellular structures in Matrigel™ for 24 hours to allow the establishment of basal polarity (Weaver et al., 2002), but not apical polarity (Fig. 5B), before digitonin permeabilization and incubation with NuMA antibodies for 3 days. After 4 days in Matrigel™, basal polarity was restored in the majority of replated S1 multicellular structures. However, apical polarity was still absent in a significant portion of these multicellular structures compared with control cultures (i.e. cells in 3D Matrigel™ for the entire culture period) (Fig. 6A). Ki67 immunostaining revealed that

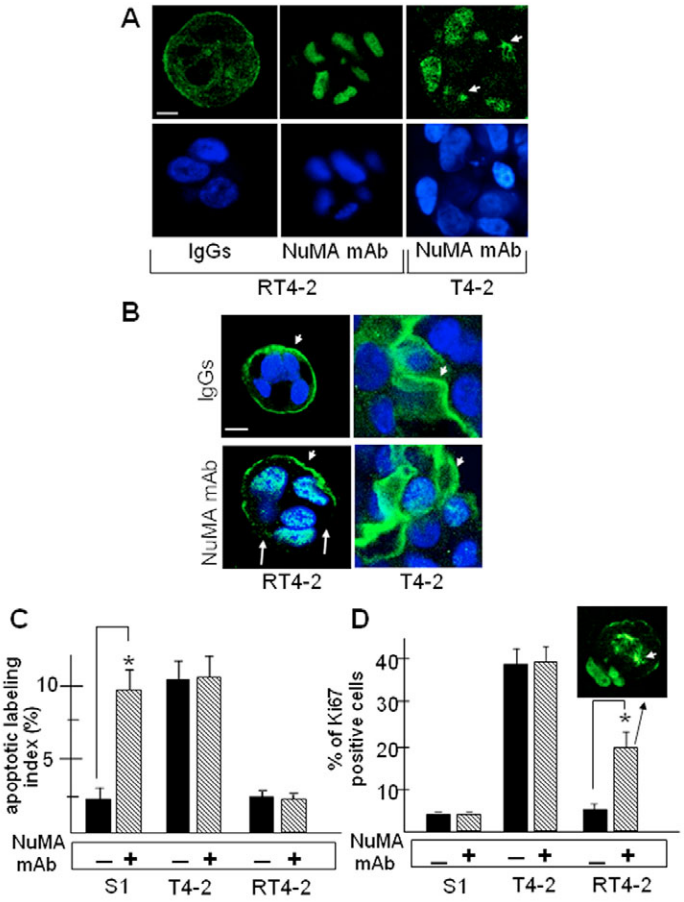

Fig. 4. Alteration of NuMA induces apoptosis in non-neoplastic S1 cells and entry into the cell cycle in reverted T4-2 cells. Non-neoplastic S1 cells and malignant T4-2 cells treated with or without the reverting agent AG1478 were cultured in 3D Matrigel™ for 10 days, followed by digitonin permeabilization and incubation with antibodies against NuMA (NuMA mAb) or nonspecific mouse immunoglobulins (IgGs) for 3 days. (A) Immunostaining with a FITC-tagged antibody against mouse IgG reveals the location of IgGs in the cytoplasm and NuMA mAb in the cell nucleus of permeabilized RT4-2 and/or T4-2 cells. Arrowheads indicate the location of NuMA at the poles of mitotic spindles in malignant cells. (B) Immunostaining for collagen IV (green, see arrowhead) in RT4-2 and T4-2 multicellular structures. Arrows indicate the lack of continuous collagen IV staining in RT4-2 cells treated with NuMA mAb. (Note that fluorescent staining for NuMA mAb can be seen in the nuclei; both collagen IV and NuMA antibodies are mouse IgG1, thus they are recognized by the same secondary antibody.) Nuclei are counterstained with DAPI (blue). (C) Histograms of the percentage of apoptotic cells. (D) Histograms of the percentage of cells in the cell cycle (Ki67-positive). Immunostaining for NuMA (green) shows evidence of mitotic spindle formation in NuMA mAb-treated RT4-2 cells (see image and arrowhead). A minimum of 300 cells were scored per replicate in three independent experiments. *P<0.05. Bars, 5 μm.

antibody-treated cultures containing a high percentage of multicellular structures lacking apical polarity had a fourfold increase in the number of Ki67-positive cells compared with NuMA antibody-treated cultures containing a high percentage of fully polarized acini (Fig. 5C, Fig. 6B). To confirm that the absence of apical polarity primes cells to enter the cell cycle

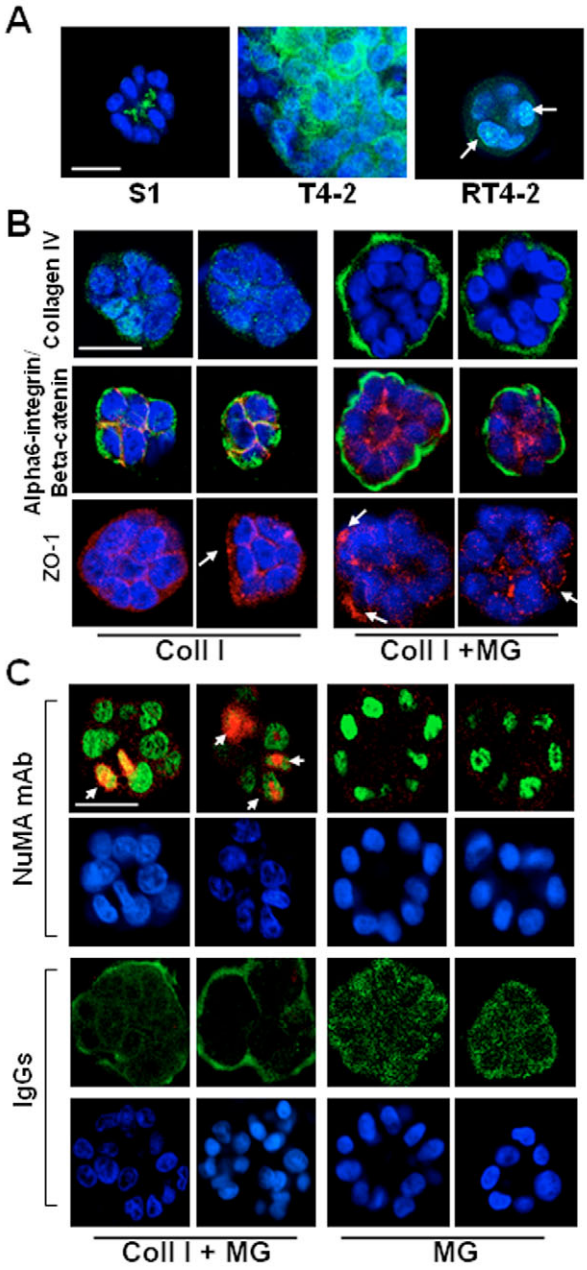

Fig. 5. S1 cells that form multicellular structures with incomplete tissue polarity are induced to enter the cell cycle upon incubation with NuMA antibodies. (A) Ten day 3D Matrigel™ culture of non-neoplastic S1, malignant T4-2 and reverted RT4-2 cells immunostained for tight junction marker ZO-1 (green). Apical polarization of S1 acini is indicated by the apical location of ZO-1. Arrows indicate the presence of ZO-1 in the nucleus of RT4-2 cells. (B) Immunostaining for collagen IV (green), α6-integrin (green), β-catenin (red) and ZO-1 (red) in non-neoplastic S1 cells cultured in collagen I for 10 days (Coll I) or cultured in collagen I for 9 days and replated in Matrigel for 24 hours (Coll I + MG). Multicellular structures in collagen I display alterations in all markers tested, as shown by the absence of continuous peripheral staining of collagen IV, the overlap of α6-integrin and β-catenin staining at cell-cell junctions – see yellow – and the diffuse location of ZO-1. By contrast, only ZO-1 staining remains altered in multicellular structures replated in Matrigel™, as shown by the presence of staining at the basal side of cells (see arrows). (C) Non-neoplastic S1 cells were cultured in Matrigel™ for 10 days to produce basoapically polarized acini (MG) or in collagen I for 9 days before replating in Matrigel™ for 24 hours (Coll I + MG) to produce a population enriched with only basally polarized multicellular structures. Acini and multicellular structures were then permeabilized with digitonin, incubated with NuMA antibodies (NuMA mAb) or nonspecific immunoglobulins (IgGs) for 3 days and immunostained for Ki67 (red) and mouse immunoglobulin (green). Immunostaining for mouse immunoglobulins highlights the nuclear location of NuMA mAb and the cytoplasmic location of nonspecific mouse IgGs. Arrows indicate Ki67-positive cells. Nuclei are counterstained with DAPI (blue). Bars, 10 μm.

regardless of the method used to alter apical polarity, we performed similar experiments with S1 acini treated with EGTA. In different cell models, it has been shown that chelation of Ca^{2+} by EGTA induces the loss of tight junction organization and thus, apical polarity (Pitelka et al., 1983; Bhat et al., 1993). Treatment of S1 acini with 1.5 mM EGTA efficiently altered apical polarity as shown by the absence of apical location of ZO-1 in the majority of the acini population after 24 hours of incubation (Fig. 6C). Following 1 hour of incubation with EGTA, plasma membranes were briefly permeabilized with digitonin and acini were incubated with antiNuMA antibody or nonspecific IgGs in the presence or absence of EGTA for 24 hours, and then in EGTA-free medium for another 48 hours. Results showed that acini treated with both EGTA and antiNuMA antibody had a fourfold increase in the number of Ki67-positive cells compared with acini treated with antiNuMA antibody only (Fig. 6D). To further assess the relationship between NuMA and tissue architecture for the control of proliferation, we used S1 cells transfected with siRNA NuMA on 2D, then replated in 3D culture 24 hours later (Abad et al., 2007), and stained for NuMA and Ki67 or NuMA and apoptosis after 8 days. This period of time is long enough to induce differentiation and still permits silencing of NuMA in a significant portion of the cell population. NuMA was absent in 14% and 28% of the cells treated with 10 nM and 50 nM of siRNA, respectively, as shown by immunostaining (Abad et al., 2007). Results indicate that silencing NuMA during the differentiation process (i.e. before full polarity can be achieved) prevents cells from exiting the cell cycle (Fig. 6E), since ~29% and ~42% of cells transfected with 10 and 50 nM NuMA siRNA show Ki67 staining, respectively, compared with ~6% in control lipofectamine, ~11% in cells transfected with 50 nM nontargeting siRNA, and ~16% of cells transfected with 50 nM GAPDH siRNA. By contrast, no increase in apoptosis was observed compared with controls (~0.6% and ~3% of apoptosis in cells transfected with 10 nM and 50 nM NuMA siRNA, respectively, compared with ~5%, ~3% and ~2.5% in cells treated with lipofectamine only, cells transfected with 50 nM nontargeting siRNA, and cells transfected with 50 nM GAPDH siRNA, respectively). Raising the concentration of NuMA siRNA to 100 nM abrogated the effect on Ki67, which suggests that the influence of silencing NuMA on the cell cycle might be counteracted with this higher concentration of siRNA upon induction of nonspecific actions (Persengiev et al., 2004). We conclude from these experiments that the degree of tissue differentiation, as measured by the status of tissue polarity, prior to induced-alteration of NuMA determines the cellular response to nuclear changes.

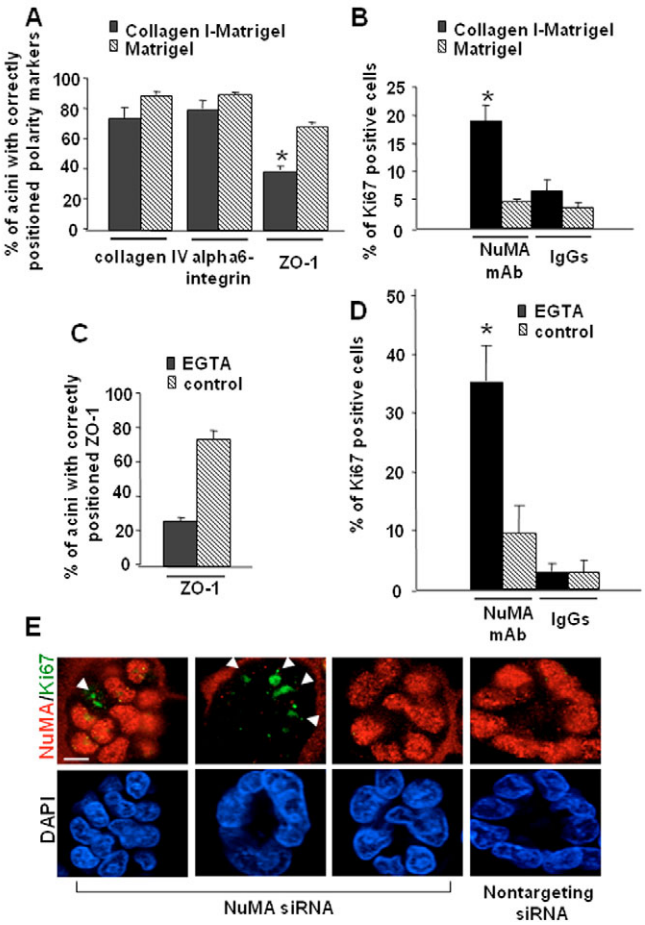

Fig. 6. Partially differentiated acini enter the cell cycle upon NuMA alteration regardless of the method used to induce incomplete polarity. (A) Histogram of the percentage of S1 multicellular structures obtained following 9 days in collagen I and 4 days in Matrigel™ (black bars) that possess intact collagen IV and α6-integrin staining, and apical location of ZO-1 compared with S1 cells cultured in Matrigel™ (shaded bars) for 13 days. (B) Non-neoplastic S1 cells were cultured in Matrigel™ for 10 days to produce basoapically polarized acini (shaded bars) or in collagen I for 9 days before replating in Matrigel™ for 24 hours (black bars) to produce a population enriched with only basally polarized multicellular structures. Acini and multicellular structures were then permeabilized with digitonin, incubated with NuMA antibodies (NuMA mAb) or nonspecific immunoglobulins (IgGs) for 3 days. Shown is the percentage of cells positive for cell cycle marker Ki67. 300 cells were scored in each replicate in three independent experiments. (C) Histogram of the percentage of S1 multicellular structures with ZO-1 apically located after treatment with EGTA for 24 hours. (D) Acini and multicellular structures were treated with EGTA for 1 hour, then briefly permeabilized with digitonin and incubated with NuMA antibodies (NuMA mAb) or nonspecific immunoglobulins (IgGs) for 3 days. EGTA was only left in the culture medium during the first 24 hours of antiNuMA antibody treatment. Shown is the percentage of cells positive for cell cycle marker Ki67. 300 cells were scored in each replicate in three independent experiments. *P<0.05. (E) Dual staining for NuMA (red) and Ki67 (green) in acini formed by cells transfected with 50 nM siRNA NuMA or 50 nM nontargeting siRNA and cultured in 3D for 8 days. Nuclei are counterstained with DAPI (blue). Arrowheads indicate strong Ki67 staining in nuclei that lack NuMA staining.

Discussion

We have shown that a significant portion of reverted malignant cells that form acinus-like structures in 3D cultures display features of higher order nuclear organization similar to those seen in differentiated non-neoplastic cells. Since reverted T4-2 malignant cells conserve an altered genome like that found in the initial malignant T4-2 cell population (Weaver et al., 1997), we propose that the loss of nuclear organization in malignant cells is linked to the loss of differentiation rather than the intrinsic non-neoplastic or neoplastic status of cells. The difference in nuclear organization observed between differentiated and malignant cells is unlikely to be the result of gross alterations in nuclear volume and shape in the cancerous stage. For example, the design of the LBF analysis allows us to measure differences in NuMA distribution that are not biased by differences in nuclear volume (Knowles et al., 2006). Moreover, the reorganization of NuMA and other nuclear proteins in reverted cells occurs although nuclei maintain an altered shape, as shown by lamin B staining. We propose that malignant reversion is a powerful means to identify features of nuclear organization that are crucial for differentiation. The current concept is that differentiation-specific nuclear structure locks the expression of genes crucial for differentiation in an off or on position (Goldman et al., 2002). It had been shown previously that the distribution of heterochromatin regions, as well as the formation of large SC35 domains coincided with the differentiation of leukemic cells (Antoniou et al., 1993; Beil et al., 2002). We show that this paradigm holds true for the tissue-like differentiation of breast epithelial cells. It is known that heterochromatin domains, such as H3K9m-rich chromocenters (Lachner et al., 2001; Maison et al., 2002), can induce the silencing of genes located in their vicinity (Brown et al., 1997), and that splicing factor speckles can stimulate the expression of genes located in their vicinity (Moen, Jr et al., 2004). Since these domains can be involved in the control of differentiation genes, it is not surprising to observe their reorganization upon induction of differentiation in tumor cells.

Differentiation of epithelial cells is dependent on the formation of a specific tissue architecture characterized by basoapical polarity. Interestingly, upon induction of the differentiation of the malignant T4-2 cells, there is only restoration of basal polarity. Because some of the major characteristics of differentiation-specific nuclear organization (i.e. perinucleolar accumulation of heterochromatin regions and formation of large SC35 domains) are restored in a significant portion of this population of reverted cells it could easily be concluded that this partial stage of differentiation is sufficient to maintain cellular homeostasis associated with normalcy. However, the experiments conducted to disrupt NuMA organization demonstrate that this is not quite the case. Although NuMA distribution seems to return to normal in reverted malignant cells, we show that the influence of altering NuMA on cell behavior (i.e. apoptosis versus proliferation) is dependent on the status of apical polarity. These data suggest that both tissue architecture and nuclear organization work in concert to control cell fate and maintain tissue homeostasis. The difference in cell behavior originates from the alteration of a nuclear protein; hence, it may be linked to a different nuclear organization between fully polarized and partially polarized acinar structures. Interestingly, we observe tight junction protein ZO-1 within the nuclei of RT4-2 cells. ZO

proteins have been previously found in the cell nucleus (Gottardi et al., 1996), notably in association with the ribonucleoprotein network (Traweger et al., 2003), where they are thought to act as regulators of gene expression (Jaramillo et al., 2004). The absence of proper apical polarity may influence nuclear structure by enabling cytoplasmic or cell membrane molecules, such as ZO-1, to concentrate in the cell nucleus, which in turn impinges on the distribution and/or function of nuclear substructures. Alternatively, it is possible that extranuclear signaling initiated by the alteration of nuclear organization triggers a different cell fate depending on the intracellular signaling network. Indeed, signaling pathways appear to organize and branch differently in nondifferentiated and differentiated cells, and specifically in cells that display or do not display apical polarity (Weaver et al., 1997; Balda et al., 2003; Ang and Constam, 2004; Liu et al., 2004).

Our findings demonstrate that the combination of alterations in tissue polarity and nuclear organization plays a crucial role in directing cells to enter the cell cycle. These data shed light on the possible mechanisms by which alterations in tissue architecture participate in cancer development. Loss of apical polarity is one of the earliest changes observed in tissue architecture in breast neoplasia (Sawada et al., 2003) (and our unpublished data). Such an alteration may represent a crucial step in the loss of tissue homeostasis that leads to uncontrolled proliferation by sensitizing cells to intracellular or extracellular factors that can impact nuclear organization and function.

Materials and Methods

Cell culture

The HMT-3522 mammary epithelial cells were cultured in H14 medium (Briand et al., 1987; Briand et al., 1996) consisting of DMEM/F12 (Gibco/BRL, St Louis, MO) with 250 ng/ml insulin (Boehringer Mannheim, Indianapolis, IN), 10 μg/ml transferrin (Sigma, St Louis, MO), 2.6 ng/ml sodium selenite (BD Biosciences, Bedford, MA), 10^{-10} M estradiol (Sigma), 1.4 μM hydrocortisone (BD Biosciences) and 5 μg/ml luteotropic hormone (Sigma). The non-neoplastic S1 cells were cultured on plastic in the presence of 10 ng/ml epidermal growth factor (EGF; BD Biosciences), and the malignant T4-2 cells were cultured on collagen type I-coated dishes (Vitrogen 100, Celtrix Laboratories, Palo Alto, CA) in the absence of EGF. H14 medium was routinely changed every 2-3 days. S1 cells and T4-2 cells were induced to recapitulate the formation of polarized glandular structures (acini) and tumor nodules, respectively, using a technique called 3D culture (Petersen et al., 1992), in which cells are plated on an exogenous extracellular matrix enriched in laminin (Matrigel™, BD Biosciences) and cultured in the presence of 5% Matrigel™ in the H14 medium. Following 7 days of 3D culture, S1 cells were induced to arrest proliferation by culturing them in H14 medium without EGF. Acinar morphogenesis, characterized by the formation of a layer of cells surrounding a lumen and delineated by an endogenous basement membrane, is routinely observed by day 8 to 10. Phenotypic reversion of T4-2 cells and formation of acinus-like structures (spheroids) was induced by culturing T4-2 cells in 3D with H14 medium containing 100 nM EGF receptor (EGFR) inhibitor Tyrphostin AG1478 (Calbiochem, San Diego, CA) or 8 μM PI3-kinase inhibitor LY294002 (Calbiochem) (Wang et al., 1998; Wang et al., 2002). AG1478 and LY294002 were dissolved in DMSO and added to the culture medium every 2 days for 10 days. Control cultures were treated with vehicle only. No significant cytotoxicity was measured during the 10-day treatment with AG1478 or LY294002.

To induce the formation of glandular structures that lack apical and basal polarity, non-neoplastic S1 cells were cultured in type I collagen (Cellagen Solution AC-5, ICN biomedicals, Costa Mesa, CA) as described previously (Weaver et al., 2002; Gudjonsson et al., 2003). Medium was changed every 2 days.

siRNA transfection

To silence NuMA during acinar differentiation, monolayers of S1 cells were transfected with 10, 50 or 100 nM siRNA NuMA (ON-TARGETplus SMARTpool, Dharmacon, Lafayette, CO) using lipofectamine (Lipofectamine™ Transfection Reagent, Invitrogen, Grand Island, NY) 24 hours before plating in 3D, as described previously (Abad et al., 2007). Controls included 50 nM nontargeting siRNA (ON-TARGETplus siCONTROL Nontargeting pool, Dharmacon), 50 nM siRNA GAPDH (ON-TARGETplus siCONTROL GAPD pool, Dharmacon) and cells treated with lipofectamine only.

Indirect immunofluorescence

Cells were cultured in four-well chamber slides (Nalge Nunc International, Naperville, IL), and incubated for 10 minutes in situ in permeabilization buffer [0.5% Triton X-100 in cytoskeleton buffer (100 mM NaCl, 300 mM sucrose, 10 mM pipes, pH 6.8, 5 mM $MgCl_2$)] with protease and phosphatase inhibitors [1 mM Pefabloc (Roche Diagnostics, Indianapolis, IN), 10 μg/ml aprotinin (Sigma), 250 μM NaF], before fixation in 4% paraformaldehyde (Sigma). Immunostaining was performed as described previously (Lelièvre et al., 1998), using mouse monoclonal antibodies against NuMA (Clone B1C11, kindly provided by Jeffrey A. Nickerson, University of Massachusetts Medical School, Worcester, MA), splicing factor SC35 (Sigma), lamin B (clone 101-B7; EMD Biosciences, San Diego, CA), promyelocytic leukemia protein (PML) (clone PG-M3; Santa Cruz Biotechnology, Santa Cruz, CA), collagen IV (clone CIV 22; DakoCytomation, Carpinteria, CA), β-catenin (clone 14; BD Biosciences), and mucin-1 (anti-human CA 15-3, clone DF3; DakoCytomation), rat polyclonal antibody against α6-integrin (clone NKI-GoH3; Chemicon, Temecula, CA), and rabbit polyclonal antibodies against H4K20m (Abcam, Cambridge, MA), H3K9m (kindly provided by Thomas Jenuwein, Research Institute of Molecular Pathology, Vienna, Austria), Ki67 (Novocastra Laboratories, Newcastle upon Tyne, United Kingdom) and ZO-1 (Zymed, Carlsbad, CA). Apoptosis was analyzed by TUNEL assay using an in situ cell death detection kit, TMR red (Roche Diagnostics). DNA was stained with 4′,6-diamidino-2-phenylindole (DAPI).

Cell permeabilization for antibody treatment

Cells were permeabilized with 0.01% digitonin in permeabilization buffer [25 mM Hepes, pH 7.2; 78 mM KHOAc, 3 mM MgHOAc, 1 mM EGTA, 300 mM sucrose, 1.0% bovine serum albumin (Sigma)], and incubated with 15 μg/ml of nonspecific mouse immunoglobulins (IgGs) (Zymed) or mouse monoclonal antibodies directed against NuMA (which induce the redistribution of endogenous NuMA) for 72 hours according to a procedure described earlier (Lelièvre et al., 1998). Then, cells were permeabilized with 0.05% Triton X-100 (Sigma) in cytoskeleton buffer including protease and phosphatase inhibitors (see Indirect Immunofluorescence) and fixed with 4% paraformaldehyde. To visualize the location of NuMA antibodies and nonspecific IgGs, treated cells were only incubated with FITC®-conjugated goat antimouse secondary antibodies (Jackson Immunoresearch, West Grove, PA) after blocking with 10% goat serum in immunofluorescence buffer (Weaver et al., 1997). NuMA antibodies are usually found in the nuclei of more than 80% of permeabilized cells. In this study, NuMA antibodies were found in more than 89% of the S1, T4-2 and RT4-2 cells. Control experiments have shown that antibodies cannot get into cells that are not permeabilized. Furthermore, treatment of cells with antiNuMA antibodies without prior cell permeabilization does not induce changes in the distribution of endogenous NuMA or in the differentiation markers (Lelièvre et al., 1998).

Imaging and data processing

Images of immunofluorescence labeling displayed in the figures were recorded using a laser scanning MRC-1024 UV (Bio-Rad Laboratories, Hemel Hampstead, UK) linked to a Diaphot 300 (Nikon, Tokyo, Japan) inverted microscope, and oil immersion 60×, numerical aperture (NA) 1.4 apochromatic and 40×, NA 1.4 fluor lenses. Optical sections were 0.2 μm. Images were converted into tiff files using Confocal Assistant™ 4.02 (Bio-Rad Laboratories, Hercules, CA) and assembled using Adobe Photoshop® 6.0 (Adobe Systems, San Jose, CA). Visual scoring of nuclear (with the exception of NuMA) and differentiation markers was performed on fluorescently immunostained 3D cultures of cells using an Olympus BX51 florescence microscope. For the radial local bright feature distribution analysis (radial-LBF) of NuMA, images containing several dozen cells in 3D culture were acquired on a Zeiss 410 confocal laser scanning microscope with a planapochromatic 63×, 1.4 NA lens. The resulting voxel dimensions of the 3D images were 0.08 μm × 0.08 μm in the plane of the slide, and 0.5 μm along the optical direction. These images were then analyzed to report the radial nuclear distribution of bright NuMA features, on a per cell basis, as previously described (Knowles et al., 2006). In this work, we calculated the integral (i) of the radial-LBF distributions function above the distribution mean, on a per nucleus basis, to assess the percentages of cells with differentiation-like and nondifferentiation-like distributions of NuMA. Since the radial-LBF distribution is normalized, the integral i is dimensionless and ranges between 0 and 1. Nuclei were then classified into four categories: $i<0.1$; $0.1\leqslant i<0.2$; $0.2\leqslant i<0.3$; and $i\geqslant 0.3$, where $i<0.1$ corresponds to a flat distribution density of NuMA (i.e., no increased concentration of bright features of staining within specific nuclear areas) as seen in the majority of malignant invasive cells. Increasing i values correspond to increasing densities of bright NuMA features, as seen when S1 cells differentiate (Knowles et al., 2006). For each image taken, the ratio of percentages of cells in the $0.1\leqslant i<0.2$ category ('differentiation-like' pattern found in the majority of acinar S1 cells) over the $i<0.1$ category ('nondifferentiation-like') was calculated. These ratios were then compared among the different cell types (i.e. S1, T4-2 and RT4-2 cells) using statistical analysis. A minimum of four images was acquired per cell type.

Statistical analysis

Data are presented as means±s.e.m. The unpaired *t*-test was used to determine the probability (*P*-value) that the sample means are equal using Prism 3.0 software. Values of $P<0.05$ were considered to be significant.

We thank Judith Campisi and Joseph Ogas for critical reading of the manuscript, and Cedric Plachot and Hibret Adissu for technical expertise and useful comments. We also thank Jeffrey Nickerson and Thomas Jenuwein for antibodies against NuMA and H3K9m, respectively. This work was supported by the Department of Defense/Breast Cancer Research Program (DMAD17-00-1-0226 and W81XHW-04-1-0670 to S.A.L.), the Walther Cancer Institute (WCI-110-114 to S.A.L.), the Lawrence Berkeley National Laboratory (subcontract 6806563 to S.A.L.), an Andrews Fellowship and a Bilsland Dissertation Fellowship (to G.C.), a Purdue Doctoral Fellowship (to P.C.A.), a Purdue Research Foundation grant (to S.A.L.), and the Purdue Cancer Center.

References

Abad, P. C., Mian, I. S., Plachot, C., Nelpurackal, A., Bator-Kelly, C. and Lelièvre, S. A. (2004). The C terminus of the nuclear protein NuMA: phylogenetic distribution and structure. *Protein Sci.* **13**, 2573-2577.

Abad, P. C., Lewis, J., Mian, I. S., Knowles, D. W., Sturgis, J., Badve, S., Xie, J. and Lelièvre, S. A. (2007). NuMA influences higher order chromatin organization in human mammary epithelium. *Mol. Biol. Cell* **18**, 348-361.

Aijaz, S., Balda, M. S. and Matter, K. (2006). Tight junctions: molecular architecture and function. *Int. Rev. Cytol.* **248**, 261-298.

Andre, C., Guillemin, M. C., Zhu, J., Koken, M. H., Quignon, F., Herve, L., Chelbi-Alix, M. K., Dhumeaux, D., Wang, Z. Y., Degos, L. et al. (1996). The PML and PML/RARalpha domains: from autoimmunity to molecular oncology and from retinoic acid to arsenic. *Exp. Cell Res.* **229**, 253-260.

Ang, S. L. and Constam, D. B. (2004). A gene network establishing polarity in the early mouse embryo. *Semin. Cell Dev. Biol.* **15**, 555-561.

Antoniou, M., Carmo-Fonseca, M., Ferreira, J. and Lamond, A. I. (1993). Nuclear organization of splicing snRNPs during differentiation of murine erythroleukemia cells in vitro. *J. Cell Biol.* **123**, 1055-1068.

Balda, M. S., Garrett, M. D. and Matter, K. (2003). The ZO-1-associated Y-box factor ZONAB regulates epithelial cell proliferation and cell density. *J. Cell Biol.* **160**, 423-432.

Barboro, P., D'Arrigo, C., Diaspro, A., Mormino, M., Alberti, I., Parodi, S., Patrone, E. and Balbi, C. (2002). Unraveling the organization of the internal nuclear matrix: RNA-dependent anchoring of NuMA to a lamin scaffold. *Exp. Cell Res.* **279**, 202-218.

Beil, M., Durschmied, D., Paschke, S., Schreiner, B., Nolte, U., Bruel, A. and Irinopoulou, T. (2002). Spatial distribution patterns of interphase centromeres during retinoic acid-induced differentiation of promyelocytic leukemia cells. *Cytometry* **47**, 217-225.

Bhat, M., Toledo-Velasquez, D., Wang, L., Malanga, C. J., Ma, J. K. and Rojanasakul, Y. (1993). Regulation of tight junction permeability by calcium mediators and cell cytoskeleton in rabbit tracheal epithelium. *Pharm. Res.* **10**, 991-997.

Bilder, D. and Perrimon, N. (2000). Localization of apical epithelial determinants by the basolateral PDZ protein Scribble. *Nature* **403**, 676-680.

Briand, P., Petersen, O. W. and Van Deurs, B. (1987). A new diploid nontumorigenic human breast epithelial cell line isolated and propagated in chemically defined medium. *In Vitro Cell. Dev. Biol.* **23**, 181-188.

Briand, P., Nielsen, K. V., Madsen, M. W. and Petersen, O. W. (1996). Trisomy 7p and malignant transformation of human breast epithelial cells following epidermal growth factor withdrawal. *Cancer Res.* **56**, 2039-2044.

Brown, K. E., Guest, S. S., Smale, S. T., Hahm, K., Merkenschlager, M. and Fisher, A. G. (1997). Association of transcriptionally silent genes with Ikaros complexes at centromeric heterochromatin. *Cell* **91**, 845-854.

Caplan, M. J. (1997). Ion pumps in epithelial cells: sorting, stabilization, and polarity. *Am. J. Physiol.* **272**, G1304-G1313.

Cereijido, M., Valdes, J., Shoshani, L. and Contreras, R. G. (1998). Role of tight junctions in establishing and maintaining cell polarity. *Annu. Rev. Physiol.* **60**, 161-177.

Chaly, N. and Munro, S. B. (1996). Centromeres reposition to the nuclear periphery during L6E9 myogenesis in vitro. *Exp. Cell Res.* **223**, 274-278.

Chrenek, M. A., Wong, P. and Weaver, V. M. (2001). Tumour-stromal interactions. Integrins and cell adhesions as modulators of mammary cell survival and transformation. *Breast Cancer Res.* **3**, 224-229.

Compton, D. A. and Cleveland, D. W. (1994). NuMA, a nuclear protein involved in mitosis and nuclear reformation. *Curr. Opin. Cell Biol.* **6**, 343-346.

Dowling, J., Yu, Q. C. and Fuchs, E. (1996). Beta4 integrin is required for hemidesmosome formation, cell adhesion and cell survival. *J. Cell Biol.* **134**, 559-572.

Fay, F. S., Taneja, K. L., Shenoy, S., Lifshitz, L. and Singer, R. H. (1997). Quantitative digital analysis of diffuse and concentrated nuclear distributions of nascent transcripts, SC35 and poly(A). *Exp. Cell Res.* **231**, 27-37.

Fischle, W., Wang, Y. and Allis, C. D. (2003). Binary switches and modification cassettes in histone biology and beyond. *Nature* **425**, 475-479.

Garagna, S., Merico, V., Sebastiano, V., Monti, M., Orlandini, G., Gatti, R., Scandroglio, R., Redi, C. A. and Zuccotti, M. (2004). Three-dimensional localization and dynamics of centromeres in mouse oocytes during folliculogenesis. *J. Mol. Histol.* **35**, 631-638.

Goldman, R. D., Gruenbaum, Y., Moir, R. D., Shumaker, D. K. and Spann, T. P. (2002). Nuclear lamins: building blocks of nuclear architecture. *Genes Dev.* **16**, 533-547.

Gonzalez-Mariscal, L. and Nava, P. (2005). Tight junctions, from tight intercellular seals to sophisticated protein complexes involved in drug delivery, pathogens interaction and cell proliferation. *Adv. Drug Deliv. Rev.* **57**, 811-814.

Gottardi, C. J., Arpin, M., Fanning, A. S. and Louvard, D. (1996). The junction-associated protein, zonula occludens-1, localizes to the nucleus before the maturation and during the remodeling of cell-cell contacts. *Proc. Natl. Acad. Sci. USA* **93**, 10779-10784.

Gribbon, C., Dahm, R., Prescott, A. R. and Quinlan, R. A. (2002). Association of the nuclear matrix component NuMA with the Cajal body and nuclear speckle compartments during transitions in transcriptional activity in lens cell differentiation. *Eur. J. Cell Biol.* **81**, 557-566.

Gudjonsson, T., Ronnov-Jessen, L., Villadsen, R., Bissell, M. J. and Petersen, O. W. (2003). To create the correct microenvironment: three-dimensional heterotypic collagen assays for human breast epithelial morphogenesis and neoplasia. *Methods* **30**, 247-255.

Hall, L. L., Smith, K. P., Byron, M. and Lawrence, J. B. (2006). Molecular anatomy of a speckle. *Anat. Rec. A Discov. Mol. Cell. Evol. Biol.* **288**, 664-675.

Jaramillo, B. E., Ponce, A., Moreno, J., Betanzos, A., Huerta, M., Lopez-Bayghen, E. and Gonzalez-Mariscal, L. (2004). Characterization of the tight junction protein ZO-2 localized at the nucleus of epithelial cells. *Exp. Cell Res.* **297**, 247-258.

Kaminker, P., Plachot, C., Kim, S. H., Chung, P., Crippen, D., Petersen, O. W., Bissell, M. J., Campisi, J. and Lelièvre, S. A. (2005). Higher-order nuclear organization in growth arrest of human mammary epithelial cells: a novel role for telomere-associated protein TIN2. *J. Cell Sci.* **118**, 1321-1330.

Knowles, D. W., Sudar, D., Bator-Kelly, C., Bissell, M. J. and Lelièvre, S. A. (2006). Automated local bright feature image analysis of nuclear protein distribution identifies changes in tissue phenotype. *Proc. Natl. Acad. Sci. USA* **103**, 4445-4450.

Lachner, M., O'Carroll, D., Rea, S., Mechtler, K. and Jenuwein, T. (2001). Methylation of histone H3 lysine 9 creates a binding site for HP1 proteins. *Nature* **410**, 116-120.

Lelièvre, S. A. and Bissell, M. J. (2005). Three dimensional cell culture: the importance of context in regulation of function. In *Encyclopedia of Molecular Cell Biology and Molecular Medicine* (Vol. 14, 2nd edn) (ed. R. A. Meyers), pp. 383-420. Weinheim: Wiley.

Lelièvre, S. A., Weaver, V. M., Nickerson, J. A., Larabell, C. A., Bhaumik, A., Petersen, O. W. and Bissell, M. J. (1998). Tissue phenotype depends on reciprocal interactions between the extracellular matrix and the structural organization of the nucleus. *Proc. Natl. Acad. Sci. USA* **95**, 14711-14716.

Liu, H., Radisky, D. C., Wang, F. and Bissell, M. J. (2004). Polarity and proliferation are controlled by distinct signaling pathways downstream of PI3-kinase in breast epithelial tumor cells. *J. Cell Biol.* **164**, 603-612.

Lochter, A., Sternlicht, M. D., Werb, Z. and Bissell, M. J. (1998). The significance of matrix metalloproteinases during early stages of tumor progression. *Ann. N. Y. Acad. Sci.* **857**, 180-193.

Maison, C., Bailly, D., Peters, A. H., Quivy, J. P., Roche, D., Taddei, A., Lachner, M., Jenuwein, T. and Almouzni, G. (2002). Higher-order structure in pericentric heterochromatin involves a distinct pattern of histone modification and an RNA component. *Nat. Genet.* **30**, 329-334.

Manuelidis, L. (1985). Indications of centromere movement during interphase and differentiation. *Ann. N. Y. Acad. Sci.* **450**, 205-221.

Martin, T. A., Watkins, G., Mansel, R. E. and Jiang, W. G. (2004). Loss of tight junction plaque molecules in breast cancer tissues is associated with a poor prognosis in patients with breast cancer. *Eur. J. Cancer* **40**, 2717-2725.

Martou, G. and De Boni, U. (2000). Nuclear topology of murine, cerebellar Purkinje neurons: changes as a function of development. *Exp. Cell Res.* **256**, 131-139.

Mitic, L. L., Schneeberger, E. E., Fanning, A. S. and Anderson, J. M. (1999). Connexin-occludin chimeras containing the ZO-binding domain of occludin localize at MDCK tight junctions and NRK cell contacts. *J. Cell Biol.* **146**, 683-693.

Moen, P. T., Jr, Johnson, C. V., Byron, M., Shopland, L. S., de la Serna, I. L., Imbalzano, A. N. and Lawrence, J. B. (2004). Repositioning of muscle-specific genes relative to the periphery of SC-35 domains during skeletal myogenesis. *Mol. Biol. Cell* **15**, 197-206.

Moir, R. D., Montag-Lowy, M. and Goldman, R. D. (1994). Dynamic properties of nuclear lamins: lamin B is associated with sites of DNA replication. *J. Cell Biol.* **125**, 1201-1212.

Nelson, C. M. and Bissell, M. J. (2006). Of extracellular matrix, scaffold, and signaling: Tissue architecture regulates development, homeostasis, and cancer. *Annu. Rev. Cell Dev. Biol.* **22**, 287-309.

O'Brien, L. E., Jou, T. S., Pollack, A. L., Zhang, Q., Hansen, S. H., Yurchenco, P. and Mostov, K. E. (2001). Rac1 orientates epithelial apical polarity through effects on basolateral laminin assembly. *Nat. Cell Biol.* **3**, 831-838.

Ortega, N. and Werb, Z. (2002). New functional roles for non-collagenous domains of basement membrane collagens. *J. Cell Sci.* **115**, 4201-4214.

Persengiev, S. P., Zhu, X. and Green, M. R. (2004). Nonspecific, concentration-dependent stimulation and repression of mammalian gene expression by small interfering RNAs (siRNAs). *RNA* **10**, 12-18.

Petersen, O. W., Ronnov-Jessen, L., Howlett, A. R. and Bissell, M. J. (1992). Interaction with basement membrane serves to rapidly distinguish growth and differentiation pattern of normal and malignant human breast epithelial cells. *Proc. Natl. Acad. Sci. USA* **89**, 9064-9068.

Pitelka, D. R., Taggart, B. N. and Hamamoto, S. T. (1983). Effects of extracellular calcium depletion on membrane topography and occluding junctions of mammary epithelial cells in culture. *J. Cell Biol.* **96**, 613-624.

Plachot, C. and Lelièvre, S. A. (2003). Novel directions in tumour biology: from basement membrane-directed polarity to DNA methylation. In *Cancer Modelling and Simulation* (ed. L. Preziosi), pp. 23-50. Boca Raton, FL: Chapman & Hall/CRC Press.

Plachot, C. and Lelièvre, S. A. (2004). DNA methylation control of tissue polarity and cellular differentiation in the mammary epithelium. *Exp. Cell Res.* **298**, 122-132.

Pullan, S., Wilson, J., Metcalfe, A., Edwards, G. M., Goberdhan, N., Tilly, J., Hickman, J. A., Dive, C. and Streuli, C. H. (1996). Requirement of basement membrane for the suppression of programmed cell death in mammary epithelium. *J. Cell Sci.* **109**, 631-642.

Rodriguez-Boulan, E. and Nelson, W. J. (1989). Morphogenesis of the polarized epithelial cell phenotype. *Science* **245**, 718-725.

Ryeom, S. W., Paul, D. and Goodenough, D. A. (2000). Truncation mutants of the tight junction protein ZO-1 disrupt corneal epithelial cell morphology. *Mol. Biol. Cell* **11**, 1687-1696.

Sawada, N., Murata, M., Kikuchi, K., Osanai, M., Tobioka, H., Kojima, T. and Chiba, H. (2003). Tight junctions and human diseases. *Med. Electron Microsc.* **36**, 147-156.

Schotta, G., Lachner, M., Sarma, K., Ebert, A., Sengupta, R., Reuter, G., Reinberg, D. and Jenuwein, T. (2004). A silencing pathway to induce H3-K9 and H4-K20 trimethylation at constitutive heterochromatin. *Genes Dev.* **18**, 1251-1262.

Shumaker, D. K., Kuczmarski, E. R. and Goldman, R. D. (2003). The nucleoskeleton: lamins and actin are major players in essential nuclear functions. *Curr. Opin. Cell Biol.* **15**, 358-366.

Traweger, A., Fuchs, R., Krizbai, I. A., Weiger, T. M., Bauer, H. C. and Bauer, H. (2003). The tight junction protein ZO-2 localizes to the nucleus and interacts with the heterogeneous nuclear ribonucleoprotein scaffold attachment factor-B. *J. Biol. Chem.* **278**, 2692-2700.

Wang, F., Weaver, V. M., Petersen, O. W., Larabell, C. A., Dedhar, S., Briand, P., Lupu, R. and Bissell, M. J. (1998). Reciprocal interactions between beta1-integrin and epidermal growth factor receptor in three-dimensional basement membrane breast cultures: a different perspective in epithelial biology. *Proc. Natl. Acad. Sci. USA* **95**, 14821-14826.

Wang, F., Hansen, R. K., Radisky, D., Yoneda, T., Barcellos-Hoff, M. H., Petersen, O. W., Turley, E. A. and Bissell, M. J. (2002). Phenotypic reversion or death of cancer cells by altering signaling pathways in three-dimensional contexts. *J. Natl. Cancer Inst.* **94**, 1494-1503.

Weaver, V. M., Petersen, O. W., Wang, F., Larabell, C. A., Briand, P., Damsky, C. and Bissell, M. J. (1997). Reversion of the malignant phenotype of human breast cells in three-dimensional culture and in vivo by integrin blocking antibodies. *J. Cell Biol.* **137**, 231-245.

Weaver, V. M., Lelièvre, S. A., Lakins, J. N., Chrenek, M. A., Jones, J. C., Giancotti, F., Werb, Z. and Bissell, M. J. (2002). beta4 integrin-dependent formation of polarized three-dimensional architecture confers resistance to apoptosis in normal and malignant mammary epithelium. *Cancer Cell* **2**, 205-216.

Zhong, S., Muller, S., Ronchetti, S., Freemont, P. S., Dejean, A. and Pandolfi, P. P. (2000). Role of SUMO-1-modified PML in nuclear body formation. *Blood* **95**, 2748-2752.

Zink, D., Fischer, A. H. and Nickerson, J. A. (2004). Nuclear structure in cancer cells. *Nat. Rev. Cancer* **4**, 677-687.